PCCP

PAPER

View Article Online
View Journal | View Issue

Cite this: *Phys. Chem. Chem. Phys.*, 2017, **19**, 29862

TMAO mediates effective attraction between lipid membranes by partitioning unevenly between bulk and lipid domains†

Shahar Sukenik, ‡ Shaked Dunsky, Avishai Barnoy, Ilan Shumilin and Daniel Harries *

Received 9th July 2017,
Accepted 19th October 2017

DOI: 10.1039/c7cp04603k

rsc.li/pccp

Under environmental duress, many organisms accumulate large amounts of osmolytes – molecularly small organic solutes. Osmolytes are known to counteract stress, driving proteins to their compact native states by their exclusion from protein surfaces. In contrast, the effect of osmolytes on lipid membranes is poorly understood and widely debated. Many fully membrane-permeable osmolytes exert an apparent attractive force between lipid membranes, yet all proposed models fail to fully account for the origin of this force. We follow the quintessential osmolyte trimethylamine *N*-oxide (TMAO) and its interaction with dimyristoyl phosphatidylcholine (DMPC) membranes in aqueous solution. We find that by partitioning away from the inter-bilayer space, TMAO pushes adjacent membranes closer together. Experiments and simulations further show that the partitioning of TMAO away from the volume between bilayers stems from its exclusion from the lipid–water interface, similar to the mechanism of protein stabilization by osmolytes. We extend our analysis to show that the preferential interaction of other physiologically relevant solutes (including sugars and DMSO) also correlates with their effect on membrane bilayer interactions. Our study resolves a long-standing puzzle, explaining how osmolytes can increase membrane–membrane attraction or repulsion depending on their preferential interactions with lipids.

Introduction

Osmolytes are naturally occurring solutes that help cells regulate osmotic pressures, thereby helping to combat environmental stresses.[1,2] Trimethylamine *N*-oxide (TMAO), a common osmolyte in marine creatures[3,4] and other biota,[5] has been extensively studied for its chemical chaperon activity: a thermodynamic stabilizing effect toward proteins and nucleic acids.[6–12] However, much less in known about the impact of TMAO on lipid bilayers, a major component of the plasma membranes, and the envelope for many cellular organelles. Many protective osmolytes and metabolite cosolutes are known to drive membranes towards one another.[13] For over four decades, this apparent attraction has been rationalized within standard models that use empirical equations of state. The apparent attraction in presence of cosolutes was then attributed in different studies to stronger van der Waals attraction, weaker hydration, or reduced undulation repulsion in the presence of cosolutes.[14–17] Yet it has been hard to find compelling experimental or theoretical evidences for these alterations, and the attractive force is thus still debated.

Extensive studies indicate that zwitterionic TMAO (Fig. 1a), whose cellular concentrations can reach several hundred millimolar, has an important osmoregulatory role[18,19] and exerts a stabilizing effect on proteins in fish and other organisms.[4,10,11,20] The overall beneficial stabilizing effect of TMAO has been linked to its effective interaction with protein interfaces.[12,21] To contrast, recent studies have shown that TMAO may have deleterious effects on human health. Specifically, elevated concentrations of TMAO in the blood (as secreted, for example, by intestinal microbiota[22]) were shown to correlate with atherosclerosis and cardiovascular disease (CVD) risks.[23–25] Lipid interactions are an important determinant in processes leading to CVD,[26] including the retention of low-density lipoprotein particles at the endothelial layer of vessel walls.[27]

As a model for lipid interactions, we examine how TMAO affects the interactions between dimyristoyl phosphatidylcholine (DMPC, Fig. 1a) bilayers in multilamellar vesicles (MLVs, shown in Fig. 1b). Using a combination of small-angle X-ray scattering (SAXS) experiments, vapor pressure osmometry (VPO), and molecular dynamic (MD) simulations, we show that TMAO acts to increase attractive interactions between DMPC

Institute of Chemistry and the Fritz Haber Research Center, The Hebrew University, Jerusalem 91904, Israel. E-mail: daniel@fh.huji.ac.il

† Electronic supplementary information (ESI) available. See DOI: 10.1039/c7cp04603k

‡ Current address: Department of Chemistry, School of Chemical Sciences, University of Illinois at Urbana-Champaign, Urbana, Illinois 61801, USA.

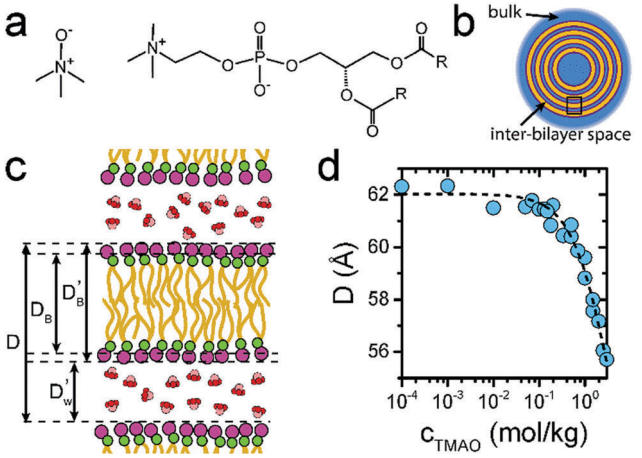

Fig. 1 TMAO reduces inter-bilayer distance in multilamellar vesicles of DMPC. (a) Schematic of TMAO (left) and DMPC (right, R represents the myristoyl $CH_3(CH_2)_{12}$ hydrocarbon chain). (b) Schematic of a multilamellar vesicle (MLV) showing the bulk solution and the inter-bilayer space. Orange color represents the hydrophobic tails, and purple represents the headgroups. The solution is shown in blue. Rectangular region is blown-up in panel (c). (c) Close-up of a membrane bilayer in an MLV highlighting the characteristic bilayer repeat distance, D, as well as the Gibbs–Luzzati bilayer (D_B) membrane (D_B') and inter-bilayer spacing (D_w'). Scheme shows phosphatidylcholine headgroups (purple and green), hydrocarbon tails (yellow), and TMAO molecules (red). Water is not shown. (d) DMPC bilayer repeat distances in MLVs as a function of TMAO concentration. Dashed line is a guide for the eye.

bilayers. As detailed in the following sections, we find that the underlying cause for the reduced distances between lipid bilayers is uneven partitioning of TMAO molecules between the lipid MLV's domain and the surrounding aqueous solution (or "bulk") domains, see schematic in Fig. 1b. Our results further show that preferential exclusion of TMAO from the lipid–water interface is responsible for the uneven partitioning. This exclusion is likely driven by unfavorable dipole orientations of TMAO molecules relative to the strongly hydrated DMPC headgroups. The net result of uneven partitioning is an effective depletion force that pushes the membranes together.

Further consolidation and analysis of previously reported data (described in the following sections) indicates that this "action at a distance" mechanism that we find for TMAO is general for many physiologically relevant solutes. Specifically, we find that it manifests in the presence of other excluded, net-neutral, membrane-permeable cosolute molecules, including sugars and DMSO. Conversely, when cosolutes are preferentially included at the membrane bilayer interface, a repulsive force emerges between lipids. Thus, we propose that uneven cosolute partitioning is a general mechanism by which cosolutes can affect lipid membranes. Specifically, our results point at an important yet often neglected physical mechanism that drives lipid membranes closer together or further apart, depending on cosolute exclusion or inclusion. Cosolute inclusion is furthermore known as important in the context of membrane freezing or desiccation, where the presence of solutes in the inter-bilayer solution can increase membrane durability and survivability.[28–31]

Although there are many differences between model bilayers and cellular membranes, the contribution of forces that emerge between lipids due to the preferential exclusion of TMAO from lipid headgroup are expected to act similarly and to augment any other interaction between more complex cellular membranes. While osmolyte concentrations are often on average small in cells and in organisms, they can locally be high, thus underlining a potentially significant effect on forces acting between lipids as well as between protein interfaces.[32] Solute preferential exclusion should therefore be considered as an important contributing force to processes of membrane remodeling, including endocytosis and fusion.

Materials and methods

Materials

TMAO (Sigma-Aldrich) was used as received, or after treating with hydrogen peroxide and recrystallization, as previously described by Russo *et al.*[33] Using both TMAO preparations gave the same results within experimental error. Highly purified (>99%) synthetic phospholipid 1,2-dimyristoyl-*sn-glycero*-3-phosphocholine (DMPC) from Avanti Polar Lipids (Alabaster, AL) was used as received in lyophilized form. Polyethylene glycol (PEG) 20k was from Sigma-Aldrich, and used as received.

Vapor pressure osmometry

The osmolality of a series of solutions containing water and TMAO and/or PEG was measured on a Wescor 5520 osmometer, as described previously for other solutes.[34–36] All measurements were performed at least in triplicates, and recalibration using 200 and 1000 mOsm standards (Wescor, Inc.) was done between each sample set. To measure the osmolarity in solutions containing lipids, the same TMAO/PEG solutions were used, but after addition of DMPC lipid. Lipid suspensions were equilibrated by 3 heat–thaw cycles (0–40 °C, 15 minutes at each temperature), sealed with parafilm, and stored for 24–48 hours before measurement. The amount of lipid and added solution were determined gravimetrically using a Mettler Toledo Excellence Plus XP microbalance. Lipid concentrations were *ca.* 300 mg ml^{-1} and those of TMAO solutions were in the range of 80–2500 mM.

Small angle X-ray scattering

Sample preparation and data acquisition followed methodology previously described.[37] In brief, lipid powder was dissolved in chloroform and dried to a thin film under nitrogen flow and then under vacuum for several hours. The lipid was then rehydrated with highly purified water (final concentration of *ca.* 30 mg ml^{-1}), TMAO aqueous solutions (0–3 M), or PEG solutions (0–40% by weight) with known concentrations and osmotic pressures, and vortexed to induce full solvation. Lipid suspensions were equilibrated by 3 heat–thaw cycles (0–40 °C, 15 minutes at each temperature), and were then stored at 4 °C. Samples were equilibrated at for at least 1 h before being X-rayed for 0.5–1 h at 30 °C. The measurements were performed using Luzzatti cells as previously described,[37] on an in-house

SAXS setup,[38] with calibration performed using silver behenate standards. Sharp, uniform scattering rings were obtained for lipid suspensions, indicative of sample homogeneity upon equilibration. The resulting 2D scattering patterns were radially integrated using Fit2D,[39] and background was subtracted (Fig. S1, ESI†). The obtained graphs showed well-defined Bragg peaks, which were fit to Gaussians (OriginPro 9.0), whose center scattering wave vector Q was used to calculate the repeat distance $D = 2\pi/Q$, determined as a function of TMAO and applied osmotic pressure. The same curves were also analyzed using more detailed models of lipid bilayers that include both the form and structure factors, implemented in the scattering analysis software X+.[40] The resulting values of repeat spacings were within 0.1 Å of those determined using simple Gaussians.

Molecular dynamics simulations

Simulations of DMPC bilayers solvated in water were run in pure water and at three different TMAO concentrations: 0.1 M, 0.5 M, and 1 M. Details of the simulation boxes are given in Table S1 (ESI†). Simulation boxes were built, hydrated, and ions were added using CHARMM-GUI membrane builder.[41] All ions were then replaced by TMAO molecules. Interactions were calculated using the CHARMM36 forcefield,[42] with TIP3P water[43] and CGenFF TMAO parameters.[44] Simulations were conducted using the NAMD package version 2.9[45] and using the *NPT* ensemble, with a 2 fs time step at T = 303.15 K and pressure of 1 bar. Temperature and pressure were kept constant using the Nose–Hoover Langevin semi-isotropic barostat[46] and Langevin thermostat algorithms.[45] Electrostatics were calculated using PME method,[47] with grid-spacing of 1 Å. van der Waals interactions were calculated with a cutoff of 12 Å and a switching distance of 10 Å. Simulation boxes were minimized for 10 000 steps, and equilibrated for 3 ns before collecting 100 ns simulation trajectories of each TMAO concentration. Analyses were performed on the last 70 ns of the simulation using VMD.[48]

Results and discussion

TMAO reduces DMPC bilayer spacing, but does not significantly modify lipid properties

We use SAXS (details in Methods) to determine the interlamellar spacing in multilamellar vesicles (MLVs) of DMPC, shown schematically in Fig. 1b and c. When placed in solutions containing TMAO and equilibrated at 30 °C, MLVs show a monotonic decrease in the characteristic bilayer repeat spacing, D, with increasing TMAO concentration (Fig. 1d).

The TMAO dependent decrease in bilayer spacing necessarily implies that the osmolyte induces a change in the balance of forces determining the interaction between the bilayers. One possibility is that the observed reduction in spacing is caused by TMAO induced changes to lipid membrane thickness, D_B (also known as the Gibbs–Luzzati bilayer thickness,[49,50] shown in Fig. 1c). We determine D_B in the presence and absence of 1 M TMAO using gravimetric measurements with decreasing lipid volume fractions, ϕ_L, and measure using SAXS the resulting membrane spacings, as detailed in ESI,† Section S1 and in ref. 50. Our results indicate that D_B derived using the gravimetric method is the same within error in the presence and absence of 1 mol kg^{-1} TMAO, Fig. 2a and b.

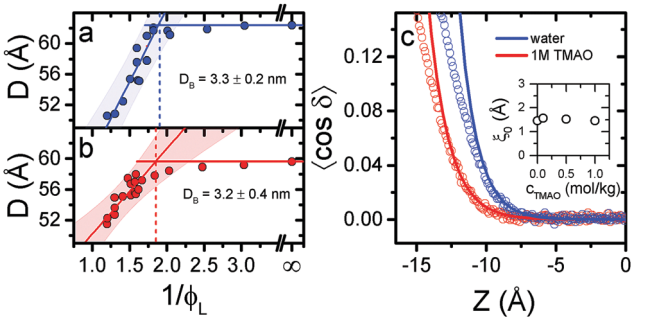

Fig. 2 Interactions between membrane and TMAO hardly affect lipid structure. (a and b) Bilayer repeat distance D *vs.* reciprocal lipid volume fraction ϕ_L as determined by SAXS. The repeat distance at low volume fractions corresponds to full hydration, while at large lipid volume fractions variations in distance indicate full uptake of added solution by the lipid. The intersection point of the two regimes allows to determine the membrane thickness D_B, which is unaltered within measurement error in the absence (a) or presence (b) of 1 mol kg^{-1} TMAO. Shaded area is 95% confidence bands of a linear fit to the initial slope of the data. See also ESI,† Section S1. (c) Decay of water orientational order $\langle\cos\delta\rangle$ *versus* distance from water midplane Z in simulations, in the presence and absence of 1 mol kg^{-1} TMAO. Inset shows that the extracted correlation lengths, ξ_0, of the order parameter for various TMAO concentrations hardly varies. Details on calculations to obtain ξ_0 are available in ESI,† Table S2. The apparent shift along Z between water and TMAO solution is directly proportional to the different solution spacings (or volume) of the simulations boxes (ESI,† Table S1).

To supplement the gravimetric method, we conducted and analyzed all-atom MD simulations of DMPC membranes in the presence and absence of increasing TMAO concentrations (see Methods and ESI,† Table S1 for details of the simulations). Like our experiments, simulations showed that the membrane thickness is roughly constant in TMAO concentrations up to 1 mol kg^{-1}, (ESI,† Table S2). In addition, estimates of membrane elasticity in the simulation derived using the splay fluctuation methodology[51] showed only a slight, *ca.* 10% increase in bilayer bending modulus, K_c, in 1 mol kg^{-1} TMAO solutions compared to the absence of TMAO (ESI,† Table S2).

To see if TMAO presence affects the arrangement of water molecules in the bilayer interface we looked for possible changes in the water molecules surrounding the lipid headgroups and their ordering in the simulations. The extent of water ordering as a function of distance from the bilayer is closely related to the so-called hydration repulsion between lipid bilayers.[52–54] This ordering depends on lipid–water interactions and can potentially impact bilayer spacing. We determined the time averaged angle of the water molecule dipole with respect to the membrane normal, $\langle\cos\delta\rangle$, as a function of distance from the solvent center of mass (*i.e.*, the "inter-membrane midplane"), Fig. 2c. Fitting the decay to a functional form proposed by Marčelja and Radić,[52,53] we find that the typical correlation distance of water orientation, ξ_0, is virtually unaffected by the presence of TMAO, as shown in the inset of Fig. 2c.

While membrane thickness remains roughly constant in the presence of TMAO in both experiments (Fig. 2a and b) and simulation (ESI,† Table S2), the average orientation of the lipid P–N lipid headgroup dipole in simulations tends to slightly larger angles with respect to the membrane normal (a change of *ca.* 1° at 1 mol kg^{-1} TMAO, see PN in ESI,† Table S2). This indicates a tendency to limit headgroup exposure to the solution in the presence of TMAO (likely due to the unfavorable interaction with TMAO, as we discuss later), and is consistent with a weak dehydrating effect of TMAO on the headgroups. Taken together, our results indicate that the considerable changes in bilayer repeat spacing (Fig. 1d) cannot be explained by the minor TMAO induced changes to membrane structure.

Reduced repeat distance caused by unequal partitioning of TMAO between bulk solution and inter-bilayer volume

Since D_B seems to be unaffected by TMAO presence, we examine the inter-bilayer solution spacing, D_w' (Fig. 1c, and ESI,† Section S2 for details; note that the corresponding value of D_B' is somewhat different than D_B[15,55]). We use the osmotic stress technique combined with SAXS to determine the values of D_w' at given osmotic pressures imposed by polyethylene glycol 20k (PEG). Since PEG is fully excluded from the lipid phase, the osmotic pressure exerted by the polymer is known. We measure D_w' at a given imposed PEG pressure in the presence of increasing concentrations of added TMAO, as shown in Fig. 3a.

The main advantage of the osmotic stress method is that the resulting isotherms have been extensively characterized by an empirical equation of state (EOS) that relates D_w' with the effective pressure exerted on the bilayer, Π_{EOS}.[14–16,56] For net-neutral membranes, the EOS is well described as a sum of three terms:

$$\Pi_{EOS} = -\frac{H}{6\pi}\frac{1}{D_w'^3} + P_h e^{-\frac{D_w'}{\lambda}} + \left(\frac{k_B T}{2\pi}\right)^2 \frac{1}{K_c}\frac{d\sigma^{-2}}{dD_w'}. \quad (1)$$

The first term represents the van der Waals (vdW) attraction between bilayers, where H is the so-called Hamaker constant, which can be determined empirically from spectroscopic measurements (see ESI,† Section S3). The second term represents hydration repulsion due to water structuring forces at the membrane interface; this exponential force has a characteristic decay length $\lambda \sim 2$ Å, and weakens significantly beyond $D_w' \sim 10$ Å. The last term in eqn (1) is due to bilayer undulations: it varies with the inverse of the membrane bending rigidity K_c, and depends linearly on the derivative of the inverse mean square fluctuation in water spacing, σ^{-2}. These fitting parameters for DMPC in water at 30 °C have previously been derived using high resolution X-ray scattering curves by Petrache *et al.*[15] (see ESI,† Table S3 for a full listing of the fit parameters and values used), and well fit our experimental results for DMPC in pure water, Fig. 3a.

Even in the absence of PEG, as TMAO concentration grows, repeat distances become smaller, see Fig. 1d. This trend is preserved also when PEG exerts additional stress, as seen in Fig. 3a.

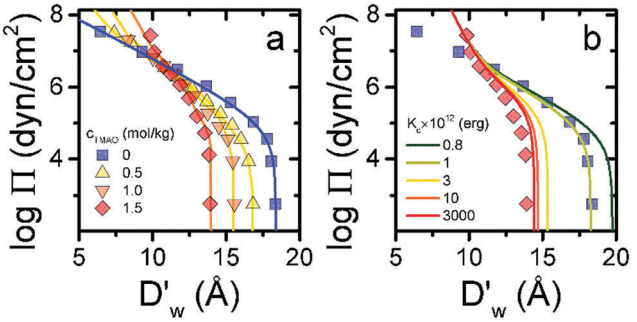

Fig. 3 Osmotic stress experiments using PEG at different TMAO concentrations. (a) PEG-exerted pressure *vs.* inter-bilayer solution spacing in the presence of increasing TMAO concentrations. Blue line is eqn (1) using the parameters in ESI,† Table S3. Other solid lines are fits using the same equation adjusted for the presence of TMAO (see text and ESI,† Sections S2–S4 for details), but with an additional term to account for the upward inflection at high pressures as described in ESI,† Section S6. (b) Values of the EOS using the parameters in ESI,† Table S3, taking the Hamaker constant to correspond to 1.5 mol kg^{-1} TMAO (ESI,† Fig. S2) and using several values for the membrane bending rigidity, to assess its effect on fit quality. EOS curves are solid lines, and are overlaid on the experimental curves in the absence (blue squares) and presence (pink diamonds) of 1.5 mol kg^{-1} of TMAO.

Considering eqn (1), there are several possible sources for this modified interaction due to TMAO. The first is the hydration interaction; however, we have shown in Fig. 2c that the typical hydration decay length ξ_0 is not expected to change considerably in the presence of TMAO, implying that the hydration force should also hardly change with TMAO addition.

The term representing vdW interactions is expected to vary with any change in dielectric response of the intervening solution, which in turn determines the value of the Hamaker constant H, as described in the ESI,† Section S3. Using known values for the dielectric response and the refractive index of TMAO solutions, we find that the Hamaker parameter decreases with increasing TMAO concentration in the lipid-intervening solvent, as shown in ESI,† Fig. S2. This would suggest a necessary weakened attraction due to TMAO that should contribute towards an increase in D_w' with TMAO addition. If taken alone, this is in clear contrast with the experimental findings, as shown by the dark green line in Fig. 3b.

Finally, we test if membrane stiffening can result in weakened repulsions that could overcome the weakened vdW attraction. Even varying the assumed value of K_c by several orders of magnitude, far beyond physically realistic values of membrane stiffness, still cannot well fit the isotherms at high TMAO concentrations (Fig. 3b). Moreover, we find in MD simulations that there is only a very slight change in K_c in the presence of TMAO, as discussed above.

We conclude that the EOS (eqn (1)) does not contain a term that can account for the force that is effectively acting to bring membranes closer in the presence of TMAO. Our focus, therefore, turns to a crucial factor that has not been considered to this point: the partitioning of TMAO between the bulk solution outside and the inter-bilayer solution inside the MLVs. We hypothesize that an effective osmotic pressure may arise due to

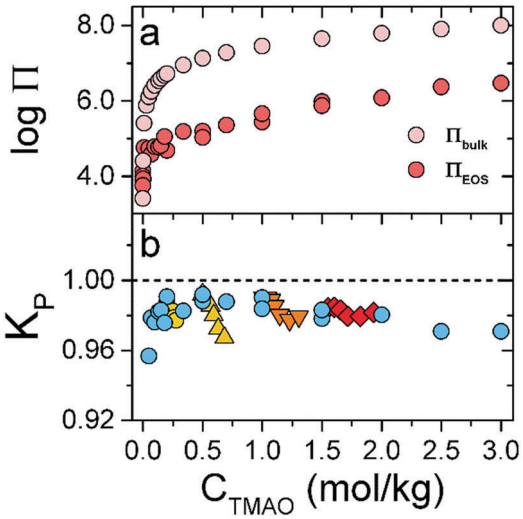

Fig. 4 TMAO partitions unevenly between lipid and bulk domains. (a) Osmotic pressure exerted by binary TMAO solutions, Π_{bulk}, and that evaluated by eqn (1), Π_{EOS}. The difference between these curves, Π_{MLV}, is in direct proportion to TMAO concentration in the inter-bilayer solution. (b) TMAO partition coefficient indicates depletion from inter-bilayer solution for all concentrations tested. Cyan circles are calculated from the curves in the absence of PEG as shown in (a). Other symbols are calculated from data in the presence of PEG (used to exert osmotic stress) for various TMAO concentrations corresponding to the colors and shapes shown in Fig. 3a. Dashed line represents hypothetical even partitioning between bulk and lipid domains.

unequal concentration between the bulk and the lipid (or inter-bilayer) space. To test this, we use the experimental inter-bilayer solution spacing D_w' to calculate the effective pressure exerted on the bilayers, Π_{EOS}, as delineated in eqn (1) and shown in Fig. 4a. Constants used in evaluating Π_{EOS} are available in ESI,† Table S3. This pressure is then subtracted from the measured osmotic pressure in lipid-free solutions, Π_{bulk} (shown for TMAO binary solutions in Fig. 4a, and for ternary solutions containing TMAO and PEG in ESI,† Fig. S3). The difference between these two pressures, $\Pi_{MLV} = \Pi_{bulk} - \Pi_{EOS}$, reports on the concentration of TMAO in the inter-bilayer solution (the lipid domain). The partition coefficient of TMAO between the bulk and the lipid phases, K_P, can be evaluated through

$$K_P = \frac{\Pi_{MLV}}{\Pi_{bulk}}. \quad (2)$$

Had TMAO partitioned evenly between the bulk and the lipid phase, the (net) pressure acting on the MLV in the absence of PEG would be $\Pi_{EOS} = 0$, and K_P would be equal to unity. Values smaller than 1 correspond to an excess of TMAO outside *vs.* inside the lipid domain. As shown in Fig. 4b, K_P is close to, but consistently lower than 1 for all concentrations tested. This value remains lower than 1 also in the presence of PEG. The deficit of TMAO in the lipid domain thus translates into an effective osmotic pressure, which pushes the membranes closer together. While this partitioning is not large, it is enough to dominate the forces acting at low PEG pressures. More precisely stated, the chemical potentials of TMAO and water in the bulk and lipid domains are necessarily equal at equilibrium. But our results indicate that this equilibrium state is reached at different inter-bilayer spacings for every TMAO concentration at the same PEG-exerted osmotic pressure. It is this difference that is due to the TMAO concentration gradient between the bulk solution and the one inside the MLVs. Furthermore, we find that K_P is not exactly constant with TMAO concentrations. Most notable, as TMAO concentration increases beyond $\sim$0.5 mol kg^{-1}, K_P becomes smaller (indicating stronger TMAO exclusion from lipids), strengthening the effective attractive force between the lipid bilayers.

The presence of PEG also apparently acts to diminish K_P (yellow-red points in Fig. 4b) but this is primarily caused by an effective increase in TMAO concentrations due to uptake of water by PEG and subsequent expected elevation in the activity coefficients of TMAO, as shown in ESI,† Fig. S3. In addition, the variation around 0.5 mol kg^{-1} in the presence of PEG could be related to uncertainties in our estimates of concentration in the lipid domain that could significantly alter our estimates of the Hamaker constant.

TMAO is depleted at the lipid membrane–water interface

What are the molecular underpinnings of the uneven partitioning of TMAO? We hypothesized that TMAO is preferentially excluded from the lipid bilayer interface, leading to its net depletion in the inter-bilayer space. We tested this by using vapor pressure osmometry to measure the preferential interaction of TMAO with the lipid bilayer. The related net number of TMAO-excluding waters per lipid, or simply "lipid preferential hydration", Γ_w, is linked to changes in osmotic pressures of TMAO solutions upon lipid addition. This methodology, developed by Courtenay *et al.*[57] for proteins and other macromolecules, relates Γ_w to the variation of the change in solution osmolality following addition of lipid membranes to solution, $\Delta\Pi_L$, with initial TMAO osmolality, Π_{TMAO}, through

$$\frac{d\Delta\Pi_L}{d\Pi_{TMAO}} = \frac{m_L}{m_w}\Gamma_w, \quad (3)$$

where m_w = 55.6 mol kg^{-1} is water molality and m_L is lipid concentration in mol kg^{-1}.[58] Fig. 5a shows that $\Delta\Pi_L$ is linear in TMAO molality, so that $\Gamma_w = 11 \pm 1$ is constant over the wide range of TMAO concentrations studied here. Positive values of Γ_w indicate preferential hydration and TMAO exclusion from lipids. Thus, we have determined that approximately 11 water molecules overall are, on average, inaccessible to TMAO for each lipid molecule at all concentrations up to $\sim$2.5 Osm. Interestingly, this number is only slightly larger than the number of so-called headgroup structural water, 8 per DMPC molecule, which is considered to be a lower limit to different measurements of tightly bound water to lipids.[49]

We compared our experimental findings with MD simulations of DMPC bilayers in aqueous solutions containing a range of TMAO concentrations (details in ESI,† Section S5). From the distribution of water and TMAO molecules as a function of their distance from the inter-bilayer solvent center of mass (Fig. 5b) we can determine the TMAO preferential hydration coefficient Γ_w per lipid molecule (see Fig. S4, ESI†). We find

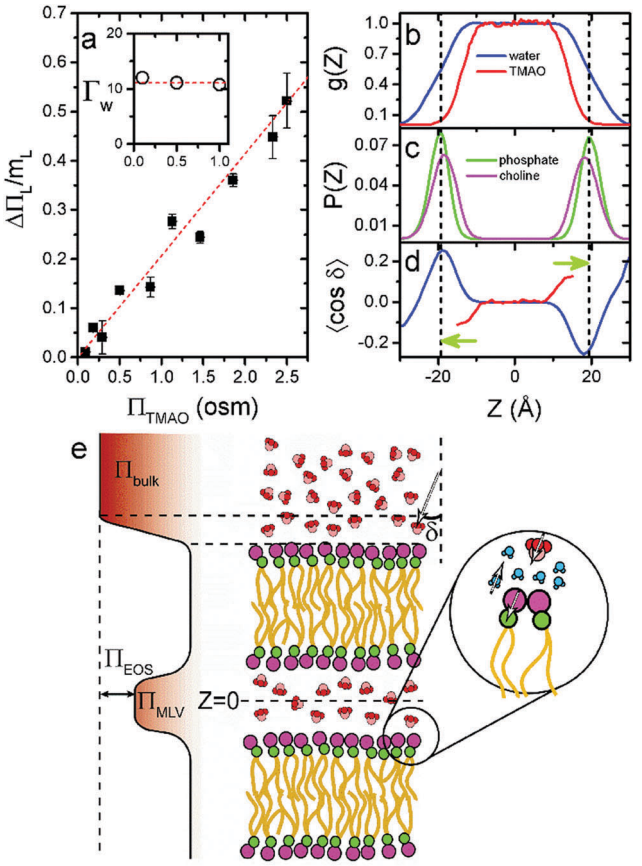

Fig. 5 Exclusion of TMAO from the lipid domain through preferential interactions with bilayer surface. (a) The change in solution osmolarity upon lipid addition changes linearly with TMAO solution osmolarity, as seen in vapor pressure osmometry. Inset shows the corresponding value calculated from MD simulations as dots (see details in ESI,† Section S5), and the dashed horizontal line is the experimental value calculated according to eqn (3). (b–d) Simulation derived pair distribution functions (b), headgroup moiety number density (c), and average dipole orientation relative to the membrane normal (d) as a function of distance from the inter-bilayer solvent mid-plane, Z. Lines represent water (blue), TMAO (red), phosphate (green) and choline (magenta). Vertical dashed lines represent average membrane bilayer position based on the phosphate headgroups. Green arrows in (d) represent the value of the average dipole between the choline and phosphate of the lipid headgroups. (e) Schematic of bulk–lipid partitioning and dipole orientation of TMAO and water in the water:DMPC:TMAO system. Red shaded area (left) represents the TMAO concentrations in the bulk and lipid (MLV) phases of the system, which are directly proportional to the osmotic pressures. The difference caused by the uneven partitioning of TMAO, pushes the bilayers closer together. Lipids are shown as green phosphates and purple cholines, with hydrocarbon tails as yellow lines. TMAO molecules are shown in red, and water molecules (in the zoomed-in region) in blue. Dipole orientations are shown as black-outlined arrows. The scheme indicates the dipole angle relative to the membrane normal, as well as the center of mass of the inter-bilayer solvent, where Z = 0.

that TMAO is preferentially excluded from the bilayer surface compared to water molecules, which in turn preferentially hydrate the headgroup layer of the membrane. In excellent agreement with the experiment, TMAO is net-excluded from *ca.* 11 water molecules around each headgroup at all concentrations tested, as calculated from the simulation and shown in the inset of Fig. 5a. The constant preferential hydration and associated net-exclusion of TMAO from the inter-bilayer space means that for the isotherms shown in Fig. 3, TMAO (average) concentrations in the lipid domain must change as osmotic pressure is increased and bilayers are pushed closer together, which also dictates an altered Hamaker constant (as discussed in ESI,† Section S3).

The finding that TMAO is excluded from the lipid interface region can be traced to the effective interaction of TMAO with the lipid headgroups, as seen in simulations. The cosine of the angle of the TMAO dipole relative to the membrane normal ($\cos\delta$) *versus* distance from the membrane (Z), Fig. 5d, shows that the dipole of the zwitterionic TMAO molecules (red line) orients itself with that of the neighbouring headgroups (value marked by green arrows). Water (blue line) intervenes between lipid and TMAO, and accordingly orients its dipole opposite to the dipoles of TMAO and lipid, thus maintaining, on average, favourable interactions with both. Fig. 5e summarizes the proposed mechanism: water orientation may act as a buffer for the unfavourable TMAO–lipid headgroup orientation, but also acts to increase the mutual TMAO–lipid exclusion beyond that expected for purely steric TMAO–lipid repulsion. This water sequestration results in depletion of TMAO from the interbilayer solution, and has previously been described in the context of osmolyte interactions with proteins in terms of a "soft" or "chemical" repulsion.[59,60]

Our results agree well with a recent spectroscopic study of TMAO interaction with DPPC monolayers at the air–water interface by Mondal.[61] There it was concluded that water dipoles oriented opposite of headgroup dipoles, and that TMAO orients oxygen-first towards the choline group, and preferentially screens the choline lipid moiety more effectively than the phosphate charge. To closely orient anti-parallel with the lipid headgroup would require further burial of TMAO into the headgroup region and displacement of hydrating waters, which overall is unfavourable. This unfavourable interaction of TMAO with the lipid headgroup region is likely also responsible for the change in the isotherm at high osmotic pressures seen at high TMAO concentrations (above $\sim$0.5 mol kg^{-1}). For these isotherms (shown in Fig. 3a), the pressure quickly rises as D_w' decreases below $\sim$11 Å. This cannot be explained by the terms in eqn (1), and fitting this data (as shown in Fig. 3a) requires an additional term discussed in the ESI,† Section S6.

Preferential cosolute exclusion drives lipid attraction while preferential inclusion promotes swelling

The correlation we find between TMAO preferential exclusion at the lipid interface and the effective attraction between membranes, shown schematically in Fig. 5e, should be a very general mechanism for cosolute action on lipids. Indeed, by analyzing previously reported studies of other cosolutes with PC lipids,[62–65] we find remarkable correlation between changes in bilayer spacing and preferential interactions Γ_s (a parameter directly related to preferential hydration, $\Gamma_s = -\Gamma_w(n_s/n_w)$, where n_s and n_w are the number of moles of solute (s) or water (w) in the sample). Fig. 6 demonstrates this correlation for

several cosolutes. All these cosolutes weaken the van der Waals interactions (since the Hamaker constant decreases), and so the EOS would predict an increase in *D*-spacing ("swelling"). However, this swelling can be reinforced or counteracted by the corresponding inclusion or exclusion of the cosolute from the lipid domain.

We find that previously reported preferential cosolute exclusion[64,65] correlates closely with reduction in bilayer repeat spacing, while cosolute inclusion is correlated with an increased swelling. Remarkably, for cosolutes such as sucrose and glucose, preferential interactions go from inclusion at low concentrations to exclusion at high concentrations, closely tracing the membrane spacing, which initially increases but then decreases, Fig. 6. At concentrations where preferential interaction vanishes (as does the osmotic pressure difference) the contribution to the van der Waals force is most relevant, and indeed increased swelling is observed. As sugar concentration grows further, preferential exclusion grows too, driving uneven partitioning. Such partitioning creates an osmotic stress that effectively attracts lipid bilayers, bringing membranes towards one another at concentrations above 1 mol kg^{-1}.

The correlation between cosolute preferential interactions and membrane spacing is analogous to the effects of similar small, non-charged cosolutes on protein folding. In these cases, preferentially included cosolutes such as urea accumulate at the protein surface and force it to unfold, whereas preferentially excluded cosolutes exert an effective depletion force driving proteins toward more compact conformations.[66,67] The self-assembled lipid membrane surface can likewise respond to the presence of cosolutes, and this may induce additional changes in MLVs that could become more prominent than any uneven partitioning. For example, cosolutes may alter membrane thickness,[65] gel-to-liquid melting temperature[68] or electrostatic interactions between bilayers.[69] Therefore, cosolute–lipid mixtures should be carefully and individually addressed to determine the net cosolute effect on the balance of forces.

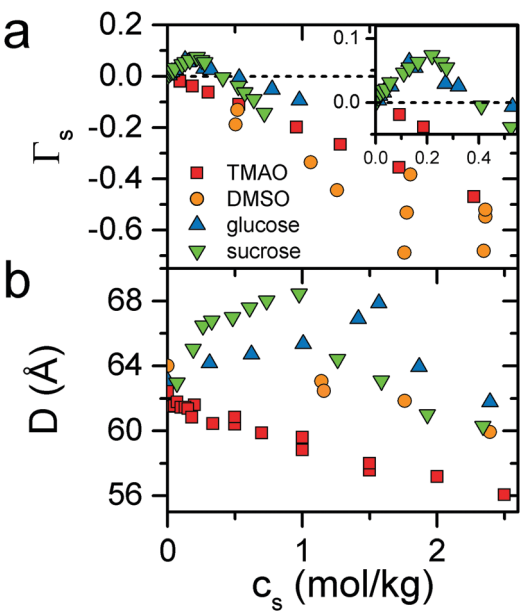

Fig. 6 Cosolute preferential interaction correlates with membrane spacing. (a) Preferential interaction of cosolute with PC lipid membrane *vs.* cosolute concentration from Westh and co-workers (for DMSO, glucose and sucrose),[64,65] and data from this study (TMAO). Dashed line represents absence of preferential interaction, while positive (negative) values indicate cosolute inclusion (exclusion). Inset zooms in on the region where glucose and sucrose turn from preferentially included to excluded. (b) Bilayer repeat spacing *D* of PC membranes *vs.* cosolute concentration c_s. DMSO data from Kisselev *et al.*,[63] sucrose and glucose data from Leneveu *et al.*,[62] and TMAO data from this study.

Concluding remarks

In this study, we showed that membranes come closer together in the presence of TMAO. This effective attraction is induced by an exclusion of TMAO from the membrane interface due to unfavorable interactions with the lipid headgroup. This preferential interaction translates into a deficit of TMAO in the lipid domain compared with the bulk solution. Membranes are thus driven closer together to minimize the volume of solution that incurs the free energy penalty associated with TMAO exclusion. Upon cosolute addition, membranes reach a new equilibrium point where repulsive forces (most notably hydration and fluctuation repulsions) balance the added effective attraction.

That solute partitioning between bulk and lipid domains can induce effective attractions is not new. A well-studied example is the driving of lipid bilayers towards one another by fully excluded polymers, such as PEG, that exert depletion forces on the lipid.[37,62] For electrolyte solutions, salt partitioning between bulk and lipid domains has long been recognized, and is routinely treated within the framework of the mean field Poisson–Boltzmann theory.[16,70] However, rarely do current models consider that net-neutral, membrane-permeable solutes can drive similar attractions or repulsions.[71] We show that unfavorable interfacial interactions between solute and lipid lead to TMAO exclusion from the lipid domain, necessarily driving lipid membranes closer. Moreover, the molecular mechanism we propose here is very general. While previously net-neutral cosolutes were often considered to either be completely excluded (as in the case of PEG[37]) or equally partitioned between the bulk and the lipid phases (as in the case of *e.g.* DMSO[13,63,72] and sugar[62]), we demonstrate the possibility for a wide range of cosolute partitioning. Such partitioning may also be relevant for other cosolutes, including the recently reported effects of buffer molecules on lipid bilayer properties.[73,74]

Although a comprehensive predictive molecular-level theory for the partitioning of net-neutral solutes is presently lacking, we anticipate that any preferentially excluded cosolute that can partition freely between membrane and bulk domains may show trends in bilayer spacing similar to TMAO and the other excluded cosolutes we have analyzed. Similarly, we showed that cosolutes that are preferentially included in the membrane domain (*viz.* sugars) correlate with an opposite force that drives membranes apart.

By bringing lipid interfaces closer together or further apart, cellular solutes may provide a non-negligible contribution to the molecular mechanisms of membrane remodeling processes. By reducing the barriers for lipid interactions, such processes may be facilitated and modulated directly by cosolute concentrations.

Conflicts of interest

There are no conflicts to declare.

Acknowledgements

We thank Dave Thirumalai for telling us about the TMAO-CVD link that inspired this study en route to a vineyard. We thank Uri Raviv for helpful discussions and for use of the SAXS setup and osmometer, and Carina Hazan for use of the microbalance. The financial support from the Israel Science Foundation (ISF grant No. 1538/13) is gratefully acknowledged. The Fritz Haber Research Center is supported by the Minerva Foundation, Munich, Germany.

References

1 P. H. Yancey, M. E. Clark, S. C. Hand, R. D. Bowlus and G. N. Somero, Living with water stress: evolution of osmolyte systems, *Science*, 1982, **217**, 1214–1222.
2 G. N. Somero and P. W. Hochachka, Biochemical Adaptation to the Environment, *Integr. Comp. Biol.*, 1971, **11**, 159–167.
3 P. H. Yancey, M. E. Gerringer, J. C. Drazen, A. Rowden and A. Jamieson, Marine fish may be biochemically constrained from inhabiting the deepest ocean depths, *Proc. Natl. Acad. Sci. U. S. A.*, 2014, **111**, 4461–4465.
4 A. J. Wang and D. W. Bolen, A naturally occurring protective system in urea-rich cells: mechanism of osmolyte protection of proteins against urea denaturation, *Biochemistry*, 1997, **36**, 9101–9108.
5 P. W. Hochachka and G. N. Somero, *Biochemical adaptation*, Oxford University Press, 2002.
6 S. S. Cho, G. Reddy, J. E. Straub and D. Thirumalai, Entropic stabilization of proteins by TMAO, *J. Phys. Chem. B*, 2011, **115**, 13401–13407.
7 J. Ma, I. M. Pazos and F. Gai, Microscopic insights into the protein-stabilizing effect of trimethylamine *N*-oxide (TMAO), *Proc. Natl. Acad. Sci. U. S. A.*, 2014, **111**, 8476–8481.
8 D. L. Pincus, C. Hyeon and D. Thirumalai, Effects of trimethylamine *N*-Oxide (TMAO) and crowding agents on the stability of RNA hairpins, *J. Am. Chem. Soc.*, 2008, **130**, 7364–7372.
9 D. Lambert, D. Leipply and D. E. Draper, The Osmolyte TMAO stabilizes native RNA tertiary structures in the absence of Mg^{2+}: evidence for a large barrier to folding from phosphate dehydration, *J. Mol. Biol.*, 2010, **404**, 138–157.
10 A. Bandyopadhyay, *et al.*, Chemical chaperones assist intracellular folding to buffer mutational variations, *Nat. Chem. Biol.*, 2012, **8**, 238–245.
11 B. J. Bennion and V. Daggett, Counteraction of urea-induced protein denaturation by trimethylamine *N*-oxide: a chemical chaperone at atomic resolution, *Proc. Natl. Acad. Sci. U. S. A.*, 2004, **101**, 6433–6438.
12 D. R. Canchi, P. Jayasimha, D. C. Rau, G. I. Makhatadze and A. E. Garcia, Molecular mechanism for the preferential exclusion of TMAO from protein surfaces, *J. Phys. Chem. B*, 2012, **116**, 12095–12104.
13 Z. W. Yu and P. J. Quinn, Phase stability of phosphatidylcholines in dimethylsulfoxide solutions, *Biophys. J.*, 1995, **69**, 1456–1463.
14 R. P. Rand and V. A. Parsegian, Hydration forces between phospholipid bilayers, *Biochim. Biophys. Acta, Rev. Biomembr.*, 1989, **988**, 351–376.
15 H. I. Petrache, *et al.*, Interbilayer interactions from high-resolution X-ray scattering, *Phys. Rev. E: Stat. Phys., Plasmas, Fluids, Relat. Interdiscip. Top.*, 1998, **57**, 7014–7024.
16 H. I. Petrache, T. Zemb, L. Belloni and V. A. Parsegian, Salt screening and specific ion adsorption determine neutral-lipid membrane interactions, *Proc. Natl. Acad. Sci. U. S. A.*, 2006, **103**, 7982–7987.
17 A. M. Schrader, C. Y. Cheng, J. N. Israelachvili and S. Han, Communication: contrasting effects of glycerol and DMSO on lipid membrane surface hydration dynamics and forces, *J. Chem. Phys.*, 2016, **145**, 041101.
18 P. W. Hochachka and G. N. Somero, *Biochemical Adaptation*, Oxford University Press, 2002, pp. 217–289.
19 I. Lidbury, J. C. Murrell and Y. Chen, Trimethylamine *N*-oxide metabolism by abundant marine heterotrophic bacteria, *Proc. Natl. Acad. Sci. U. S. A.*, 2014, **111**, 2710–2715.
20 J. A. Raymond, Seasonal variations of trimethylamine oxide and urea in the blood of a cold-adapted marine teleost, the rainbow smelt, *Fish Physiol. Biochem.*, 1994, **13**, 13–22.
21 E. Schneck, D. Horinek and R. R. Netz, Insight into the molecular mechanisms of protein stabilizing osmolytes from global force-field variations, *J. Phys. Chem. B*, 2013, **117**, 8310–8321.
22 Z. Wang, *et al.*, Gut flora metabolism of phosphatidylcholine promotes cardiovascular disease, *Nature*, 2011, **472**, 57–63.
23 A. Martínez-del Campo, K. A. Romano, F. E. Rey and E. P. Balskus, The Plot Thickens: Diet Microbe Interactions May Modulate Thrombosis Risk, *Cell Metab.*, 2016, **23**, 573–575.
24 Z. Wang, *et al.*, Gut flora metabolism of phosphatidylcholine promotes cardiovascular disease, *Nature*, 2011, **472**, 57–63.
25 R. Koeth, *et al.*, Intestinal microbiota metabolism of l-carnitine, a nutrient in red meat, promotes atherosclerosis, *Nat. Med.*, 2013, **19**, 576–585.
26 A. J. J. Wood and R. H. Knopp, Drug Treatment of Lipid Disorders, *N. Engl. J. Med.*, 1999, **341**, 498–511.
27 D. J. Rader, Regulation of reverse cholesterol transport and clinical implications, *Am. J. Cardiol.*, 2003, **92**, 42J–49J.

28 B. Kent, *et al.*, Direct Comparison of Disaccharide Interaction with Lipid Membranes at Reduced Hydrations, *Langmuir*, 2015, **31**, 9134–9141.
29 G. Bryant, K. L. Koster and J. Wolfe, Membrane behaviour in seeds and other systems at low water content: the various effects of solutes, *Seed Sci. Res.*, 2001, **11**, 17–25.
30 G. Bryant and J. Wolfe, *Trends in Colloid and Interface Science*, Steinkopff, 1993, pp. 187–187.
31 J. H. Crowe, L. M. Crowe, J. F. Carpenter and C. Aurell Wistrom, Stabilization of dry phospholipid bilayers and proteins by sugars, *Biochem. J.*, 1987, **242**, 1–10.
32 M. B. Burg and J. D. Ferraris, Intracellular Organic Osmolytes: Function and Regulation, *J. Biol. Chem.*, 2008, **283**, 7309–7313.
33 A. T. Russo, J. Rösgen and D. W. Bolen, Osmolyte Effects on Kinetics of FKBP12 C22A Folding Coupled with Prolyl Isomerization, *J. Mol. Biol.*, 2003, **330**, 851–866.
34 V. Parsegian, R. P. Rand, N. Fuller and D. C. Rau, *Methods Enzymol.*, 1986, **127**, 400–416.
35 M. Poplinger, I. Shumilin and D. Harries, Impact of trehalose on the activity of sodium and potassium chloride in aqueous solutions: why trehalose is worth its salt, *Food Chem.*, 2017, **237**, 1209–1215.
36 E. S. Courtenay, M. W. Capp and M. T. T. Record Jr, Thermodynamics of interactions of urea and guanidinium salts with protein surface: relationship between solute effects on protein processes and changes in water-accessible surface area, *Protein Sci.*, 2001, **10**, 2485–2497.
37 H. I. Petrache, D. Harries and V. A. Parsegian, *Methods in Molecular Biology*, Humana Press, 2007, vol. 400, pp. 405–419.
38 M. Nadler, *et al.*, Following the structural changes during zinc-induced crystallization of charged membranes using time-resolved solution X-ray scattering, *Soft Matter*, 2011, **7**, 1512–1523.
39 A. Hammersley, FIT2D: an introduction and overview, in *European Synchrotron Radiation Facility Internal Report ESRF97HA02T*, 1997, pp. 1–33.
40 T. Ben-Nun, A. Ginsburg, P. Székely and U. Raviv, X+: a comprehensive computationally accelerated structure analysis tool for solution X-ray scattering from supramolecular self-assemblies, *J. Appl. Crystallogr.*, 2010, **43**, 1522–1531.
41 E. L. Wu, *et al.*, CHARMM-GUI membrane builder toward realistic biological membrane simulations, *J. Comput. Chem.*, 2014, **35**, 1997–2004.
42 J. Huang and A. D. Mackerell, CHARMM36 all-atom additive protein force field: validation based on comparison to NMR data, *J. Comput. Chem.*, 2013, **34**, 2135–2145.
43 W. L. Jorgensen, J. Chandrasekhar, J. D. Madura, R. W. Impey and M. L. Klein, Comparison of simple potential functions for simulating liquid water, *J. Chem. Phys.*, 1983, **79**, 926–935.
44 K. Vanommeslaeghe, *et al.*, CHARMM general force field: a force field for drug-like molecules compatible with the CHARMM all-atom additive biological force fields, *J. Comput. Chem.*, 2009, **31**, 671–690.
45 J. C. Phillips, *et al.*, Scalable molecular dynamics with NAMD, *J. Comput. Chem.*, 2005, **26**, 1781–1802.
46 S. Nosé and M. L. Klein, Constant pressure molecular dynamics for molecular systems, *Mol. Phys.*, 1983, **50**, 1055–1076.
47 U. Essmann, *et al.*, A smooth particle mesh Ewald method, *J. Chem. Phys.*, 1995, **103**, 8577–8593.
48 W. Humphrey, A. Dalke and K. Schulten, VMD: visual molecular dynamics, *J. Mol. Graphics Modell.*, 1996, **14**, 33–38.
49 S. Tristram-Nagle, *Membrane Hydration, Subcellular Biochemistry*, 2015, vol. 71, pp. 1–16.
50 E. Leontidis, A. Aroti, L. Belloni, M. Dubois and T. Zemb, Effects of monovalent anions of the hofmeister series on DPPC lipid bilayers Part II: modeling the perpendicular and lateral equation-of-state, *Biophys. J.*, 2007, **93**, 1591–1607.
51 G. Khelashvili, B. Kollmitzer, P. Heftberger, G. Pabst and D. Harries, Calculating the bending modulus for multicomponent lipid membranes in different thermodynamic phases, *J. Chem. Theory Comput.*, 2013, **9**, 3866–3871.
52 S. Marčelja and N. Radić, Repulsion of interfaces due to boundary water, *Chem. Phys. Lett.*, 1976, **3**, 129–130.
53 E. Schneck, F. Sedlmeier and R. R. Netz, Hydration repulsion between biomembranes results from an interplay of dehydration and depolarization, *Proc. Natl. Acad. Sci. U. S. A.*, 2012, **109**, 14405–14409.
54 V. A. Parsegian and T. Zemb, Hydration forces: observations, explanations, expectations, questions, *Curr. Opin. Colloid Interface Sci.*, 2011, **16**, 618–624.
55 J. F. Nagle and S. Tristram-Nagle, Structure of lipid bilayers, *Biochim. Biophys. Acta*, 2000, **1469**, 159–195.
56 G. Pabst, S. Danner, R. Podgornik and J. Katsaras, Entropy-driven softening of fluid lipid bilayers by alamethicin, *Langmuir*, 2007, **23**, 11705–11711.
57 E. S. Courtenay, M. W. Capp, C. F. Anderson and M. T. Record Jr., Vapor pressure osmometry studies of osmolyte-protein interactions: implications for the action of osmoprotectants *in vivo* and for the interpretation of 'osmotic stress' experiments *in vitro*, *Biochemistry*, 2000, **39**, 4455–4471.
58 D. Harries, D. C. Rau and V. A. Parsegian, Solutes probe hydration in specific association of cyclodextrin and adamantane, *J. Am. Chem. Soc.*, 2005, **127**, 2184–2190.
59 L. Sapir and D. Harries, Is the depletion force entropic? Molecular crowding beyond steric interactions, *Curr. Opin. Colloid Interface Sci.*, 2015, **20**, 3–10.
60 M. Sarkar, C. Li and G. J. Pielak, Soft interactions and crowding, *Biophys. Rev.*, 2013, **5**, 187–194.
61 J. A. Mondal, Effect of Trimethylamine *N*-Oxide on Interfacial Electrostatics at Phospholipid Monolayer–Water Interfaces and Its Relevance to Cardiovascular Disease, *J. Phys. Chem. Lett.*, 2016, **7**, 1704–1708.
62 D. M. M. LeNeveu and R. P. Rand, Measurement and modification of forces between lecithin bilayers, *Biophys. J.*, 1977, **18**, 209–230.
63 M. A. Kiselev, P. Lesieur, A. M. Kisselev, C. Grabielle-Madelmond and M. Ollivon, DMSO-induced dehydration

of DPPC membranes studied by X-ray diffraction, small-angle neutron scattering, and calorimetry, *J. Alloys Compd.*, 1999, **286**, 195–202.

64 P. Westh, Preferential interaction of dimethyl sulfoxide and phosphatidyl choline membranes, *Biochim. Biophys. Acta*, 2004, **1664**, 217–223.

65 H. D. Andersen, C. Wang, L. Arleth, G. H. Peters and P. Westh, Reconciliation of opposing views on membrane–sugar interactions, *Proc. Natl. Acad. Sci. U. S. A.*, 2011, **108**, 1874–1878.

66 S. Sukenik, L. Sapir and D. Harries, Balance of enthalpy and entropy in depletion forces, *Curr. Opin. Colloid Interface Sci.*, 2013, **18**, 495–501.

67 L. Sapir and D. Harries, Macromolecular compaction by mixed solutions: bridging versus depletion attraction, *Curr. Opin. Colloid Interface Sci.*, 2016, **22**, 80–87.

68 S. Tristram-Nagle, T. Moore, H. I. Petrache and J. F. Nagle, DMSO produces a new subgel phase in DPPC: DSC and X-ray diffraction study, *Biochim. Biophys. Acta, Biomembr.*, 1998, **1369**, 19–33.

69 H. I. Petrache, I. Kimchi, D. Harries and V. A. Parsegian, Measured depletion of ions at the biomembrane interface, *J. Am. Chem. Soc.*, 2005, **127**, 11546–11547.

70 D. Ben-Yaakov, D. Andelman, D. Harries and R. Podgornik, Beyond standard Poisson-Boltzmann theory: ion-specific interactions in aqueous solutions, *J. Phys.: Condens. Matter*, 2009, **21**, 424106.

71 F. O. Costa-Balogh, H. Wennerström, L. Wadsö and E. Sparr, How Small Polar Molecules Protect Membrane Systems against Osmotic Stress: The Urea–Water–Phospholipid System, *J. Phys. Chem. B*, 2006, **110**, 23845–23852.

72 C.-Y. Cheng, J. Song, J. Pas, L. H. H. Meijer and S. Han, DMSO Induces Dehydration near Lipid Membrane Surfaces, *Biophys. J.*, 2015, **109**, 330–339.

73 M. M. Koerner, *et al.*, Electrodynamics of lipid membrane interactions in the presence of zwitterionic buffers, *Biophys. J.*, 2011, **101**, 362–369.

74 M. A. Johnson, S. Seifert, H. I. Petrache and A. C. Kimble-Hill, Phase coexistence in single-lipid membranes induced by buffering agents, *Langmuir*, 2014, **30**, 9880–9885.